HHS Public Access

Author manuscript

Biochim Biophys Acta. Author manuscript; available in PMC 2016 May 01.

Published in final edited form as:

Biochim Biophys Acta. 2015 May ; 1851(5): 527–536. doi:10.1016/j.bbalip.2015.01.012.

Lipid abnormalities in alpha/beta2-syntrophin null mice are independent from ABCA1

Tobias Hebel[a], **Kristina Eisinger**[a], **Markus Neumeier**[a], **Lisa Rein-Fischboeck**[a], **Rebekka Pohl**[a], **Elisabeth M. Meier**[a], **Alfred Boettcher**[b], **Stanley C. Froehner**[c], **Marvin E. Adams**[c], **Gerhard Liebisch**[b], **Sabrina Krautbauer**[a], and **Christa Buechler**[a,§]

[a]Department of Internal Medicine I, Regensburg University Hospital, Regensburg, Germany

[b]Institute for Clinical Chemistry and Laboratory Medicine, Regensburg University Hospital, Regensburg, Germany

[c]Department of Physiology and Biophysics, University of Washington, Washington, USA

Abstract

The syntrophins alpha (SNTA) and beta 2 (SNTB2) are molecular adaptor proteins shown to stabilize ABCA1, an essential regulator of HDL cholesterol. Furthermore, SNTB2 is involved in glucose stimulated insulin release. Hyperglycemia and dyslipidemia are characteristic features of the metabolic syndrome, a serious public health problem with rising prevalence. Therefore, it is important to understand the role of the syntrophins herein. Mice deficient for both syntrophins (SNTA/B2−/−) have normal insulin and glucose tolerance, hepatic ABCA1 protein and cholesterol. When challenged with a HFD, wild type and SNTA/B2−/− mice have similar weight gain, adiposity, serum and liver triglycerides. Hepatic ABCA1, serum insulin and insulin sensitivity are normal while glucose tolerance is impaired. Liver cholesterol is reduced, and expression of SREBP2 and HMG-CoA-R is increased in the knockout mice. Scavenger receptor-BI (SR-BI) protein is strongly diminished in the liver of SNTA/B2−/− mice while SR-BI binding protein NHERF1 is not changed and PDZK1 is even induced. Knock-down of SNTA, SNTB2 or both has no effect on hepatocyte SR-BI and PDZK1 proteins. Further, SR-BI levels are not reduced in brown adipose tissue of SNTA/B2−/− mice excluding that syntrophins directly stabilize SR-BI. SR-BI stability is regulated by MAPK and phosphorylated ERK2 is induced in the liver of the knock-out mice. Blockage of ERK activity upregulates hepatocyte SR-BI showing that increased MAPK activity contributes to low SR-BI. Sphingomyelin which is well described to regulate cholesterol metabolism is reduced in the liver and serum of the knock-out mice while the size of serum lipoproteins is not affected. Current data exclude a major function of these

[§]Corresponding author: Christa Buechler, PhD; Tel.:+49-941-944-7009, Fax.:+49-941-944-7019, christa.buechler@klinik.uni-regensburg.de.

Declaration of interest

The authors declare that there is no conflict of interest that could be perceived as prejudicing the impartiality of the research reported.

syntrophins in ABCA1 activity and insulin release but suggest a role in regulating glucose uptake, ERK and SR-BI levels, and sphingomyelin metabolism in obesity.

Keywords

scavenger receptor B-I; liver; glucose tolerance test; insulin; sphingomyelin

Introduction

Obesity is a main risk factor for several common diseases including cardiovascular disease, and non-alcoholic fatty liver disease (NAFLD) [1, 2]. Insulin resistance, hyperinsulinemia, and low levels of HDL are characteristic features associated with obesity [3]. HDL metabolism is largely controlled by hepatic ATP binding cassette transporter A1 (ABCA1) which regulates the generation of nascent HDL particles and scavenger receptor-BI (SR-BI) mediating the delivery of HDL cholesterol to the liver [4–6].

SR-BI and ABCA1 protein are stabilized by the post synaptic density protein (PSD95), Drosophila disc large tumor suppressor (Dlg1), and zonula occludens-1 protein (zo-1) (PDZ) proteins PDZK1 and syntrophins, respectively [4, 7]. Hepatic SR-BI protein is strongly reduced in PDZK1 deficient mice and abnormally large, cholesterol rich HDL particles circulate in plasma [8]. SR-BI in the adrenal gland is not affected in PDZK1 knock-out mice demonstrating a tissue specific function of this complex [8].

Hepatic ABCA1 deficiency does not only reduce serum HDL but also low density lipoprotein (LDL) [5]. The four carboxy terminal amino acids of ABCA1 bind to the PDZ domains of the syntrophin isoforms alpha (SNTA), beta 1 (SNTB1) and beta 2 (SNTB2). SNTA delays the degradation of ABCA1, and thereby, stimulates apolipoprotein A-I (ApoA-I) mediated release of cholesterol. Association of ABCA1 and SNTB2 has been confirmed by different approaches and the complex is found in the liver, platelets, and macrophages. Knock-down of SNTB2 modestly lowers lipid efflux suggesting a minor role of SNTB2 in ABCA1 biology. SNTB1 stabilizes ABCA1 protein in the macrophages and the liver [4]

Syntrophins are well described components of the skeletal muscle dystrophin associated protein complex (DAPC) and connect various transporters and extracellular proteins with the actin cytoskeleton [9]. SNTA/B2 −/− animals have fewer folds at the neuromuscular junctions, reduced levels of acetylcholine receptors and ran shorter distances on voluntary exercise wheels [10].

Binding of the granule protein islet cell antigen (ICA) 512 to the PDZ domain of SNTB2 anchors insulin transporting vesicles to actin filaments and restrains their mobility. Glucose causes destabilization of this complex and subsequent exocytosis of insulin suggesting a role of SNTB2 in postprandial glucose clearance [9, 11].

Low HDL cholesterol and impaired glucose metabolism are characteristic features of the metabolic syndrome and major risk factors in the pathogenesis of atherosclerotic diseases,

type 2 diabetes and NAFLD [1, 2]. Therefore, it is of importance to understand the physiological relevance of SNTA and SNTB2 in ABCA1 function and insulin release which was analyzed herein using mice which lack SNTA and SNTB2 [10].

Materials and Methods

Cell culture, chemicals and antibodies

Hepa 1-6 cells were purchased from the American Type Culture Collection (ATCC, Manassas, VA, USA). Cells were cultivated at 37°C and 5% CO_2 in DMEM medium with 10% FBS and 1% penicillin/streptomycin. EndoPorter was ordered from GeneTools (Philomath, OR, USA). Syntrophin isoform specific antibodies have been described elsewhere [12]. Antibodies specific for caveolin-1, Cox-IV, β-actin, AMPK, pAMPK, Akt, ERK1/2, pERK1/2 and GAPDH were from New England Biolabs GmbH (Frankfurt am Main, Germany). ABCA1 specific antibody was from Abcam (Cambridge, UK). ELISAs for ApoB and ApoA-I were ordered from Hölzel Diagnostika (Köln, Germany). ApoA-I antibody was from AMS Biotechnology (Abingdon, U.K.) and ApoE antibody from Merck Chemicals GmbH (Schwalbach, Germany). MnSOD, NHERF1 and SMS2 antibodies were from Thermo Fisher Scientific (Schwerte, Germany). SR-BI antibody was from Biomol (Hamburg, Germany). CD36 antibody was from Acris Antibodies (Herford, Germany). SREBP2 antibody was ordered from Cayman Chemicals (IBL International GmbH, Hamburg, Germany). The ERK1/2 inhibitor PD98059 was from Calbiochem (Darmstadt, Germany) and cells were incubated with 20 μM of the inhibitor for 24 h. Adiponectin ELISA, PDZK1 antibody, chemerin specific antibody and ELISA were for R&D Systems (Wiesbaden, Germany). Insulin was determined by an ELISA from Mercodia (Uppsala, Sweden). Hematoxylin, Eosin and Sirius Red were ordered from Roth (Karlsruhe, Germany).

Primary human cells

Human liver tissue for cell isolation was obtained from liver resections of patients undergoing partial hepatectomy for metastatic liver tumors of colorectal cancer. Experimental procedures were performed according to the guidelines of the charitable state controlled foundation Human Tissue and Cell Research (HTCR), with the written informed patient’s consent approved by the local ethical committee of the University of Regensburg. Isolation and cultivation of the cells has been recently described [13].

Quantification of lipids

Triglyceride concentrations were measured using GPO-PAP micro-test (purchased from Roche, Mannheim, Germany). Liver cholesterol was determined by an assay from Diaglobal (Berlin, Germany). Serum lipids, hepatic sphingomyelin and ceramide were quantified by direct flow injection electrospray ionization tandem mass spectrometry (ESI-MS/MS) in positive ion mode using the analytical setup and strategy as described previously [13, 14].

Animal studies

Animal studies have been approved by the local committees on animal research of the University of Washington or the University of Regensburg. Animal procedures were in accordance with the EU Directive 2010/63/EU for animal experiments.

Wild type and STNA/B2−/− mice in the respective groups were matched for age. Liver tissue of 3 male C57BL/6 control mice and 3 mice deficient in SNTA and SNTB2 kept on a standard diet (SD) was used for immunoblot analysis. Furthermore, serum and liver tissue of 8 C57BL/6 and 8 SNTA/B2−/− male mice kept on a high fat diet (HFD) for 25 weeks were used. Gross energy of HFD (ssniff® EF R/M acc. D12451 (II) mod.) was 22.1 MJ / kg, 35% of kJ were from carbohydrate, 20% from protein and 45% from fat (Ssniff, Soest, Germany). Detailed list of fatty acid composition can be found at the homepage of the company.

Intraperitoneal glucose (IPGTT) and insulin tolerance (IPITT) tests

Mice on a SD were fasted for 16 h, fasting glucose was determined and 1 mg/g body weight glucose was injected intraperitoneally. Blood glucose values were obtained at 15, 30, 60 and 120 min after glucose injection. IPGTT was performed using 6 male C57BL/6 control mice (body weight 23.6 ± 0.9 g) and 3 male SNTA/B2−/− mice (body weight 24.2 ± 0.7 g, $p = 0.548$). Fasting insulin was measured in the serum of 9 male wild type (25.8 ± 5.8 g body weight) and 10 male SNTA/B2−/− (27.0 ± 2.7 g body weight, $p = 0.905$) mice.

Male mice fed a HFD for 16 weeks were fasted for 12 h, fasting glucose was determined and 1 mg/g body weight glucose was injected intraperitoneally. Blood glucose values were obtained at 15, 30, 60, 90 and 120 min. IPGTT was performed using 5 male C57BL/6 control mice (body weight 35.0 ± 2.7 g) and 5 male SNTA/B2−/− mice (body weight 31.6 ± 2.5 g, $p = 0.095$). Serum insulin was measured in 5 wild type animals (34.2 ± 2.6 g body weight) and 4 SNTA/B2−/− mice (31.6 ± 2.5 g body weight, $p = 0.149$).

Mice on a SD were fasted for 4 h, fasting glucose was determined and 1.0 mU/g body weight of insulin was injected intraperitoneally. Blood glucose values were obtained at 15, 30, 60, and 120 min after insulin injection. IPITT was performed using 6 male C57BL/6 control mice (body weight 23.7 ± 1.8 g) and 3 male SNTA/B2−/− mice (body weight 24.8 ± 1.2 g, $p = 0.381$). Male mice fed a HFD for 16 weeks were fasted for 4 h and 1.0 mU/g body weight of insulin was injected intraperitoneally. Blood glucose values were obtained at 0, 15, 30, 60, 90 and 120 min after insulin injection. IPITT was performed using 5 male C57BL/6 control mice (body weight 37.4 ± 2.1 g) and 5 male SNTA/B2−/− mice (body weight 32.2 ± 3.4 g, $p = 0.032$).

Immunoblotting

Immunoblotting was perfomed as described [15]. Quantification was done using ImageJ software [16].

Immunoprecipitation

For immunoprecipitation the Pierce™ Classic Magnetic IP/Co-IP Kit was used. Shortly, 1 mg liver tissue was incubated with 10 µl SR-BI antibody. IP Lysis/Wash Buffer provided in

the kit was supplemented with proteinase and phosphatase inhibitors. Elution was performed using the Lane Marker Sample Buffer from the Kit and 35 µl of the eluate was separated by SDS-PAGE.

Separation of Lipoproteins by Nondenaturing Gradient Gel Electrophoresis and Western Blotting

Plasma samples were mixed with an equal volume of native sample buffer and 5 µl were separated by 4 to 16% polyacrylamide gradient gel electrophoresis in native running buffer (Invitrogen, Carlsbad, CA). Electrophoresis was carried out at 60 V constant voltage at 10°C for 18 h. Separated lipoproteins were electrotransferred to polyvinylidene difluoride membranes. Plasma samples were prestained with a lipophilic dialkylaminostyryl fluorophore (N-(3-Sulfopropyl)-4-(4-(didecylamino)styryl)pyridinium, inner salt [Di_{10}-ASP-PS] (Molecular Probes)). Fluorescent-stained lipoproteins were detected with a Typhoon scanner (GE Healthcare) and analyzed with ImageQuant software (GE Healthcare).

ApoA-I and ApoE-containing lipoproteins were detected by Western blot analysis with polyclonal antibodies against mouse ApoA-I (PAB 10089, Abnova) and ApoE (ab947, Chemicon). Molecular weights (particle sizes) were determined using High Molecular Weight Native Marker Kit (GE Healthcare: thyroglobulin (669 kDa, 17 nm), ferritin (440 kDa, 12.2 nm), catalase (232 kDa, 9.2 nm), lactate dehydrogenase (140 kDa, 8.1 nm), and bovine serum albumin (67 kDa, 7.1 nm)).

Transfection of cell lines

Silencer® Select Pre-Designed siRNAs and Silencer Negative Control siRNA were from Applied Biosystems (Darmstadt, Germany). Three different siRNAs (Suppl. Table 1) were pooled to knock-down SNTA or SNTB2, respectively. To knock-down both syntrophins, cells were transfected with the six different siRNAs. EndoPorter was used for transfection as recommended by the company. Cells were harvested 48 h after transfection.

Monitoring of Gene Expression by Real-time RT-PCR

Total RNA was isolated with TRIzol reagent from Life Technologies GmbH (Darmstadt, Germany) and 1 µg RNA was reverse transcribed using the Promega Reverse Transcription System (Promega, Madison, WI) in a volume of 40 µl; 2 µl of the cDNA was used for amplification in glass capillaries (LightCycler) with the primers listed in Suppl. Table 2. These oligonucleotides were synthesized by Metabion (Planegg-Martinsried, Germany). Real-time PCR was performed using the LightCycler FastStart DNA Master SYBR Green I kit (Roche, Mannheim, Germany) and the specificity of the PCRs was confirmed by sequencing of the amplified DNA fragments (Geneart, Regensburg, Germany). For quantification of the results, RNA of liver tissue was reverse transcribed, cDNA was serially diluted and used to create a standard curve for each of the genes analyzed. The second derivative maximum method was used for quantification with the LightCycler software. Values were normalized to cyclophilin mRNA expression.

Immunohistochemistry

Immunohistochemical studies for the expression of PDZK1 utilized the EnVision+ Kit (DAKO, Glostrup, Denmark) based on a HRP labeled polymer which is conjugated with a secondary antibody. Three μm sections were cut from formalin-fixed and paraffin-embedded mouse liver tissues. After deparaffinization for 15 min in Histol, tissue sections were rehydrated in descending ethanol series following antigen retrieval (microwave oven for 20 min at 800 W in sodium citrate buffer). Endogenous peroxidase activity was eliminated by subsequent incubation with 0.3% hydrogen peroxide for 10 min. After washing in TBS, 0.5% Tween 20 slides were incubated for 1 h in a protein-blocking solution (DAKO). Incubation with the PDZK1 antibody was performed overnight at 4°C in a humid chamber. After thorough washing with TBS, 0.5% Tween 20, tissue sections were incubated with anti-goat HRP labeled polymer for 30 min. Staining was completed by incubation with DAB substrate chromogen (DAKO) according to the manufacturer's instructions.

Statistical analysis

Data are given as mean ± SD (SPSS Statistics 21.0 program, IBM, Leibniz Rechenzentrum, München, Germany). Statistical differences were analyzed by two-tailed Mann-Whitney U Test (SPSS Statistics 21.0 program). Paired data were analyzed with MS Excel. A value of $p < 0.05$ was regarded as significant.

Results

Hepatic ABCA1 and serum cholesterol are normal in SNTA/B2−/− mice fed a standard diet (SD)

The syntrophins alpha (SNTA), beta 1 (SNTB1) and beta 2 (SNTB2) have been shown to affect ABCA1 activity partly by stabilizing ABCA1 protein [4]. To find out whether deficiency of SNTA and SNTB2 is associated with reduced expression of this transporter, ABCA1 was analyzed by immunoblot in the liver tissues of wild type and SNTA/B2 null mice fed a SD. ABCA1 was similarly expressed in the liver of wild type and double knock-out mice (Fig. 1A). SNTB1 was not changed in the liver of SNTA/B2 null mice (Fig. 1A). Further, SR-BI and apolipoprotein E (ApoE) proteins which have a role in HDL metabolism [17] were normally abundant (Fig. 1A). These findings suggest that ABCA1 protein levels were not affected by the absence of SNTA and SNTB2 *in vivo*. To evaluate whether hepatic ABCA1 activity is impaired, serum cholesterol and apoB-100 which are reduced in mice with liver ABCA1 deficiency [5] were measured. Cholesterol and apoB-100 were similarly concentrated in serum of wild type and SNTA/B2−/− mice (Fig. 1B and data not shown).

Systemic insulin, glucose tolerance and insulin sensitivity are normal in SNTA/B2 −/− mice fed a SD

SNTB2 regulates glucose stimulated insulin release in pancreatic beta-cells [11]. To identify whether glucose induced insulin production is impaired intraperitoneal glucose tolerance test (IPGTT) was performed. Glucose clearance was modestly delayed in the knock-out mice and this difference was significant 2 h after glucose injection (Fig. 1C). Area under the curve (AUC) for glucose during IPGTT was modestly higher in the null mice (Fig. 1D). Serum

insulin measured 30 min after glucose injection was similar in wild type and SNTA/B2−/− mice (Fig. 1E). To assess insulin sensitivity blood glucose was measured after injection of insulin and was comparable in wild type and SNTA/B2−/− mice during the 2 h follow up (Fig. 1F). Glucose AUC for IPITT and fasting insulin were similar in both mouse strains (Fig. 1G, H). Hence, deficiency of these syntrophins did not cause gross abnormalities in cholesterol and glucose homeostasis at least when the animals were fed a SD.

High fat diet (HFD) fed mice are commonly used to study obesity which is associated with disturbed glucose and lipid metabolisms [1–3]. This model was employed to investigate whether these syntrophins affect insulin and cholesterol levels in metabolically stressed animals.

Body weight gain, adiposity, and triglycerides are normal in SNTA/B2−/− mice on a HFD

Animals were fed a HFD for 25 weeks. Food uptake was 2.9 ± 0.3 g/day/animal in 7 wild type and 3.1 ± 0.4 g/day/animal in 5 knock-out mice (data not shown). Wild type and SNTA/B2−/− gained similar weight and final body weight was comparable (Fig. 2A). To assess adiposity, weight of subcutaneous, epididymal and perirenal fat pads were determined and were found to be similar in wild type and SNTA/B2−/− mice (data not shown). In accordance with similar fat pad weights, serum adiponectin and chemerin were not altered (Fig. 2B, C). Liver weight was normal and neither hepatic nor systemic triglycerides were increased (Fig. 2D – F). Liver histology did not reveal any gross abnormalities. Liver steatosis was similar in wild type and knock-out mice and fibrosis was hardly detectable in the liver of both strains (Fig. 2G).

Impaired glucose tolerance and normal systemic insulin and hepatic ABCA1 in SNTA/B2 −/− mice fed a HFD

IPGTT was performed in mice fed a HFD for 16 weeks. Glucose was less efficiently cleared in the SNTA/B −/− mice (Fig. 3A, B). Fasting insulin and insulin sensitivity were comparable (Fig. 3C, D). ABCA1 protein and mRNA were similarly expressed in the liver of wild type and SNTA/B2 −/− mice fed a HFD for 25 weeks (Fig. 3E, F, G). NAFLD is associated with reduced abundance of the mitochondrial proteins manganese superoxide dismutase (MnSOD) and cytochrome c oxidase/complex IV (Cox-IV) in the liver [18, 19] while CD36 is increased [20]. These proteins were normally expressed in the knock-out mice (Fig. 3E) further suggesting that liver function is similarly affected in obesity in both genotypes. SNTB1 was not induced in the liver of SNTA/B−/− animals (Fig. 3E) excluding compensatory induction of this related adapter protein.

ApoA-I, the major apolipoprotein of HDL [4], was not altered in serum (Fig. 3H, I) and liver mRNA expression was similar to wild type animals (Fig. 3J). ApoB-100 serum levels and liver mRNA expression were comparable in wild type and SNTA/B2−/− mice (Fig 3K, L).

Hepatic cholesterol is reduced in SNTA/B2−/− mice fed a HFD

Hepatic cholesterol was nevertheless reduced in the SNTA/B2−/− mice (Fig. 4A). SREBP2 is a physiologically important transcription factor regulating genes involved in cholesterol synthesis and uptake [21]. Yet, expression of SREBP2 mRNA and protein and HMG-CoA-

R mRNA was significantly increased (Fig. 4B, C, D, E). LDL-R expression was not regulated (Fig. 4F). To find out whether other proteins with a function in hepatic cholesterol metabolism were affected [22, 23] expression of phosphorylated and total AMP-activated protein kinase (AMPK), Akt and caveolin-1 was analyzed and was found to be unchanged (Fig. 4G, H). Chemerin, which is increased in rodent and human NAFLD liver [24, 25], was similarly abundant in wild type and SNTA/B2−/− animals (Fig. 4H).

Hepatic SR-BI is reduced in SNTA/B2−/− mice fed a HFD

SR-BI mediates uptake of HDL cholesterol and overexpression of SR-BI in the liver is associated with elevated hepatic cholesterol demonstrating a critical function of this protein in hepatic cholesterol homeostasis [26]. Indeed, SR-BI protein was strongly downregulated in the liver of SNTA/B2 knock-out mice (Fig. 5A, B). SR-BI mRNA levels were comparable to the wild type mice (Fig. 5C). PDZK1 which stabilizes SR-BI protein in the liver [7] was significantly increased (Fig. 5A, D). Na+/H+ exchanger regulatory factor 1 (NHERF1) downregulates SR-BI [27] but was not induced in the liver of SNTA/B2−/− mice (Fig. 5A). Cholesterol 7 alpha-hydroxylase (CYP7A1), a key enzyme in bile acid synthesis thereby regulating hepatic cholesterol levels [28], was normally expressed (Fig. 5E).

To analyze SR-BI in extrahepatic tissues SR-BI protein was determined in brown adipose tissue of the mice fed a HFD for 25 weeks, but here levels were normal (Fig. 5F, G). To explore whether low SNTA, SNTB2 or both directly cause reduced SR-BI or increased PDZK1, hepatocytes were treated with siRNAs to knock-down SNTA, SNTB2 or both. SNTA and SNTB2 were strongly reduced in the cells treated with the respective siRNAs but SR-BI and PDZK1 were not changed (Fig. 5H). Localisation of PDZK1 in the liver was determined by immunohistochemistry and was not altered in the knock-out mice (Fig. 5I). PDZK1 was found associated with SR-BI in the liver of wild type and knock-out mice by immunoprecipitation (Fig. 5J) showing that complex formation is not impaired in the SNTA/B−/− mice. SNTA was not precipitated by the SR-BI antibody (Fig. 5J).

ERK1/2 regulates SR-BI protein stability [29] and its expression was induced in SNTA-B−/− mice liver (Fig. 6A, B). Phosphorylated ERK2 but not ERK1 was significantly increased (Fig. 6C and data not shown). Inhibition of ERK1/2 by PD98059 in primary human hepatocytes was associated with higher SR-BI protein (Fig. 6D, E) while ABCA1 was not altered (data not shown). This suggests that increased ERK2 activity in the liver of SNTA/B−/− mice contributes to lower SR-BI protein.

Serum cholesterol is normal in SNTA/B2−/− mice fed a HFD

Serum cholesterol of SNTA/B2−/− mice fed a HFD was nevertheless found unchanged (Fig. 7A). Major cholesteryl ester species (CE 18:2, 18:3, 20:3, and 20:4) were not altered (data not shown). Since in mice acyl coenzyme A: cholesteryl acyltransferase (ACAT) prefers saturated and monounsaturated fatty acids for esterification and lecithin-cholesterol acyltransferase (LCAT) prefers polyunsaturated fatty acids, the distribution of saturated and monounsaturated with polyunsaturated fatty acids in CE was compared by calculating the ratio of saturated + monounsaturated on polyunsaturated CE [30, 31]. This ratio was decreased in the SNTA/B2 null mice (Fig. 7B). The minor species CE 16:0, 20:1, 22:1, and

22:4 were lower and CE 18:1 tended to be reduced in the serum of the knock-out mice (data not shown).

Sphingomyelin (SM) is a highly abundant serum lipid shown to affect cholesterol esterification and uptake by the liver [31–33]. In serum of SNTA/B2−/− mice SM was strongly reduced (Fig. 7C) while ceramides were not altered (Fig. 7D). Remarkably, in the liver SM was also lower and ceramide tended to be increased (Fig. 7E, F) suggesting that sphingomyelinase or sphingomyelinsynthase activity may be changed. The mRNA and protein levels of sphingomyelin synthase 2, the major sphingomyelin synthase isoform in the liver [34], were normal (Fig. 7G; H) while mRNA of sphingomyelin phosphodiesterase 3 (SMPD3) tended to be increased (Fig. 7I).

ApoA-I and ApoE containing lipoproteins are normal in the SNTA/B2−/− mice

Plasma was separated by native polyacrylamide electrophoresis. Staining of lipoproteins by a lipophilic fluorophore, and immunoblot analysis of ApoA-I and ApoE did not reveal any significant abnormalities in the knock-out mice (Fig. 8A–C). The HDL particles with a size of about 10 nm tended to be increased in the SNTA/B2−/− mice (Fig. 8D).

Discussion

SNTB2 is involved in insulin granule localization and vesicle release in the pancreatic INS-1 cells [11]. Despite this *in vitro* evidence suggesting an essential role of this adaptor protein in systemic insulin levels no abnormalities have been found in mice lacking SNTA and SNTB2 fed a SD. This excludes a physiologically important function of these adaptor proteins in glucose induced insulin release. Though it is still possible that other family members compensate for the deficiency of SNTB2, a function of further syntrophins in pancreatic β-cells has not been described so far [9].

SNTA and SNTB2 PDZ-domains bind to the last four carboxy-terminal amino acids of ABCA1 and this complex increases ABCA1 stability and subsequently lipid efflux [4]. ABCA1 is, however, normally expressed in the liver of mice deficient in SNTA and SNTB2. Serum cholesterol, ApoA-I and ApoB-100 which are all influenced by hepatic ABCA1 [5] are normal. Therefore, syntrophins are of no importance in ABCA1 function. This *in vivo* finding is in accordance with *in vitro* data. Recombinant ABCA1 with a C-terminally added GFP tag can’t bind to syntrophins [35, 36] but is functional [37]. Deletion of the last four carboxy-terminal amino acids neither affects ABCA1 protein levels nor grossly impairs its lipid efflux capacity [38]. These and current *in vivo* findings argue against a role of C-terminally bound PDZ proteins for ABCA1 stability and activity.

Obesity is the consequence of unbalanced energy intake and wastage [39]. SNTA/B2 deficient mice show abnormalities in skeletal muscle tissue and exercise less [10]. To investigate whether the knock-out mice are prone to obesity development because of reduced physical activity the animals were fed a HFD. However, both strains respond similarly to this metabolic stress. Body weight, fat pad weight, systemic and hepatic chemerin, serum adiponectin, serum insulin, serum and hepatic triglycerides are normal. SNTA/B −/− mice on a HFD display impaired glucose clearance while insulin sensitivity is

not affected. This shows that glucose uptake of peripheral tissues is impaired while suppression of hepatic glucose synthesis by insulin is normal. Whether this is related to defects in glucose uptake transporters in skeletal muscle and /or adipose tissue needs further studies. Hepatic expression of the mitochondrial proteins MnSOD, Cox-IV and CD36 which are affected in obesity [18–20] is similar in wild type and SNTA/B2 null mice.

While serum cholesterol is normal hepatic cholesterol is lower in the knock-out animals. Subsequently, SREBP2 and HMG-CoA-R are upregulated. Most likely because of the high inter-individual variability in mRNA levels an induction of LDL-R mRNA expression has not been identified.

Several molecules regulating hepatic cholesterol metabolism including AMPK and caveolin-1 [22, 23] are not changed in the liver of SNTA/B2−/− mice. SR-BI protein is, however, markedly reduced. SR-BI is involved in selective uptake of HDL-cholesterol and subsequently serum cholesterol is increased in SR-BI deficient mice [40]. Serum cholesterol is normal in SNTA/B2−/− mice and distribution of ApoE and ApoA-I containing lipoprotein particles is comparable in the wild type and the knock-out mice. Therefore, reduction of SR-BI by about 80% is not associated with marked changes in serum lipoproteins. This is in line with findings in PDZK1 deficient mice whose hepatic SR-BI is less than 5% of wild type mice. Despite this low expression of SR-BI in the PDZK1 deficient animals serum cholesterol is about 100 mg/dl lower compared to SR-BI deficient mice [7]. This suggests that about 20% residual expression of SR-BI in the liver is not associated with altered serum cholesterol and / or HDL particle size. Mice studied herein have been kept on a HFD. Liver-specific overexpression of murine SR-BI markedly lowers serum cholesterol. These changes are less pronounced when these animals are fed a HFD [26] demonstrating that other pathways influencing serum cholesterol levels become increasingly important in obesity. Accordingly, SR-BI is about two-fold induced in the liver of wild type mice fed a HFD while plasma HDL-cholesterol and LDL-cholesterol are even increased [41, 42].

These findings suggest that reduced liver cholesterol is not a consequence of low SR-BI levels. SR-BI is important in biliary cholesterol release [43] but whether biliary cholesterol is changed in the null mice has not been analyzed. At least expression of the bile acid synthesis enzyme CYP7a1 [28] is not altered.

Sphingomyelin levels are closely related to cellular cholesterol concentrations. Sphingomyelin is a constituent of all lipoproteins and affects HDL-mediated cholesterol efflux, hepatic cholesterol uptake, clearance of triglyceride rich remnants, aggregation and binding of LDL to the aterial wall [44–46]. Further research is needed to clarify whether reduced hepatic cholesterol is a consequence of low sphingomyelin in these animals. Sphingomyelin content is regulated by sphingomyelin synthases and sphingomyelin synthase 2 is the major isoform in the liver [34] and is not lower in the SNTA/B2−/− mice. SMPD3 mRNA tends to be increased and enzyme activity has to be measured in future studies. Analysis of single cholesteryl ester species suggests that activity of hepatic ACAT is reduced. Ceramide which tends to be increased in the liver of the knock-out mice has been shown to inhibit ACAT activity [47] and thereby may affect cholesteryl ester species levels in the knock-out mice.

Whether low sphingomyelin contributes to reduced SR-BI has not been clarified. Hepatic overexpression of sphingomyelin synthases 1 and 2 induces liver SR-BI expression [48] while treatment of hepatoma cells with sphingomyelinase does not affect SR-BI protein (own unpublished results). Recently it has been shown that ERK1/2 regulates SR-BI protein stability in HuH7 hepatocytes by a mechanism involving ligand-independent activation of PPARα [29]. ERK1/2 and phosphorylated ERK2 are increased in SNTA/B2−/− liver. This MAPK exerts various functions and its activity is enhanced by multiple stimuli [49] which will be identified in ongoing studies. Inhibition of ERK1/2 in primary hepatocytes induces SR-BI protein. This suggests that ERK2 contributes to low SR-BI in the liver of SNTA/B2−/− mice. The MAPK pathway activates PPARα in hepatocytes [50] but whether PPARα is involved herein has not been studied. In accordance with the literature [51] activation of PPARα by fenofibrate lowers SR-BI in primary hepatocytes (data not shown). SR-BI protein is normally expressed in brown adipose tissues of SNTA/B2−/− mice fed a HFD suggesting that it is not universally reduced in all tissues.

Knock-down of SNTA, SNTB2 or both syntrophins in hepatoma cells does not affect SR-BI protein. However, cell lines are at least not appropriate to study the role of PDZK1 in SR-BI protein expression. Here, the effects of PDZK1 on SR-BI protein levels are independent of SR-BI's C-terminus, and thus do not occur via the mechanism identified in vivo [52]. The C-terminal amino acids of SR-BI (EAKL) do not represent a class I PDZ binding motif needed for complex formation with syntrophins [4, 7, 27] and SNTA does not bind SR-BI.

SR-BI in hepatocytes is stabilized by forming a complex with the PDZ domains of PDZK1 while overexpression of Na^+/H^+ exchanger regulatory factors (NHERFs) 1 and 2 downregulates SR-BI protein [7, 27]. NHERF1 is not altered in the liver of the null mice and PDZK1 protein is even induced in the liver tissue of the SNTA/B2−/− mice. Cellular localization of PDZK1 in the liver and binding of PDZK1 to SR-BI are not affected by SNTA/SNTB2 deficiency. This excludes that low SR-BI in SNTA/B2 deficient mice on a HFD is explained by disturbed association with this adaptor protein.

This is to our knowledge the first study analyzing the role of SNTA/B2 deficiency in lipid and glucose metabolisms. The current findings show a function of these adaptor proteins in hepatic cholesterol homeostasis in obesity which is independent of ABCA1.

Supplementary Material

Refer to Web version on PubMed Central for supplementary material.

Acknowledgments

Funding

The study was supported by a grant of the German Research Foundation (BU 1141/8-1) and the NIH (NS33145).

References

1. Buechler C, Wanninger J, Neumeier M. Adiponectin, a key adipokine in obesity related liver diseases. World J Gastroenterol. 2011; 17:2801–2811. [PubMed: 21734787]

2. Haffner SM. Relationship of metabolic risk factors and development of cardiovascular disease and diabetes. Obesity (Silver Spring). 2006; 14(Suppl 3):121S–127S. [PubMed: 16931493]
3. Hjermann I. The metabolic cardiovascular syndrome: syndrome X, Reaven's syndrome, insulin resistance syndrome, atherothrombogenic syndrome. Journal of cardiovascular pharmacology. 1992; 20(Suppl 8):S5–10. [PubMed: 1283771]
4. Buechler C, Bauer S. ATP binding cassette transporter A1 (ABCA1) associated proteins: potential drug targets in the metabolic syndrome and atherosclerotic disease? Current pharmaceutical biotechnology. 2012; 13:319–330. [PubMed: 21470122]
5. Chung S, Timmins JM, Duong M, Degirolamo C, Rong S, Sawyer JK, Singaraja RR, Hayden MR, Maeda N, Rudel LL, Shelness GS, Parks JS. Targeted deletion of hepatocyte ABCA1 leads to very low density lipoprotein triglyceride overproduction and low density lipoprotein hypercatabolism. J Biol Chem. 2010; 285:12197–12209. [PubMed: 20178985]
6. Zannis VI, Chroni A, Krieger M. Role of apoA-I, ABCA1, LCAT, and SR-BI in the biogenesis of HDL. J Mol Med (Berl). 2006; 84:276–294. [PubMed: 16501936]
7. Yesilaltay A, Kocher O, Pal R, Leiva A, Quinones V, Rigotti A, Krieger M. PDZK1 is required for maintaining hepatic scavenger receptor, class B, type I (SR-BI) steady state levels but not its surface localization or function. J Biol Chem. 2006; 281:28975–28980. [PubMed: 16867981]
8. Kocher O, Yesilaltay A, Cirovic C, Pal R, Rigotti A, Krieger M. Targeted disruption of the PDZK1 gene in mice causes tissue-specific depletion of the high density lipoprotein receptor scavenger receptor class B type I and altered lipoprotein metabolism. J Biol Chem. 2003; 278:52820–52825. [PubMed: 14551195]
9. Bhat HF, Adams ME, Khanday FA. Syntrophin proteins as Santa Claus: role(s) in cell signal transduction. Cellular and molecular life sciences : CMLS. 2013 Jul; 70(14):2533–2554. [PubMed: 23263165]
10. Adams ME, Kramarcy N, Fukuda T, Engel AG, Sealock R, Froehner SC. Structural abnormalities at neuromuscular synapses lacking multiple syntrophin isoforms. J Neurosci. 2004; 24:10302–10309. [PubMed: 15548643]
11. Ort T, Voronov S, Guo J, Zawalich K, Froehner SC, Zawalich W, Solimena M. Dephosphorylation of beta2-syntrophin and Ca2+/mu-calpain-mediated cleavage of ICA512 upon stimulation of insulin secretion. Embo J. 2001; 20:4013–4023. [PubMed: 11483505]
12. Peters MF, Adams ME, Froehner SC. Differential association of syntrophin pairs with the dystrophin complex. J Cell Biol. 1997; 138:81–93. [PubMed: 9214383]
13. Eisinger K, Krautbauer S, Hebel T, Schmitz G, Aslanidis C, Liebisch G, Buechler C. Lipidomic analysis of the liver from high-fat diet induced obese mice identifies changes in multiple lipid classes. Exp Mol Pathol. 2014; 97:37–43. [PubMed: 24830603]
14. K, Eisinger; Liebisch, G.; Schmitz, G.; Aslanidis, C.; Krautbauer, S.; Buechler, C. Lipidomic analysis of serum from high fat diet induced obese mice. International journal of molecular sciences. 2014; 15:2991–3002. [PubMed: 24562328]
15. Bauer S, Wanninger J, Schmidhofer S, Weigert J, Neumeier M, Dorn C, Hellerbrand C, Zimara N, Schaffler A, Aslanidis C, Buechler C. Sterol regulatory element-binding protein 2 (SREBP2) activation after excess triglyceride storage induces chemerin in hypertrophic adipocytes. Endocrinology. 2011; 152:26–35. [PubMed: 21084441]
16. Schneider CA, Rasband WS, Eliceiri KW. NIH Image to ImageJ: 25 years of image analysis. Nature methods. 2012; 9:671–675. [PubMed: 22930834]
17. Kawashiri MA, Maugeais C, Rader DJ. High-density lipoprotein metabolism: molecular targets for new therapies for atherosclerosis. Current atherosclerosis reports. 2000; 2:363–372. [PubMed: 11122767]
18. Handa P, Maliken BD, Nelson JE, Morgan-Stevenson V, Messner DJ, Dhillon BK, Klintworth HM, Beauchamp M, Yeh MM, Elfers CT, Roth CL, Kowdley KV. Reduced adiponectin signaling due to weight gain results in nonalcoholic steatohepatitis through impaired mitochondrial biogenesis. Hepatology. 2014; 60:133–145. [PubMed: 24464605]
19. Krautbauer S, Eisinger K, Lupke M, Wanninger J, Ruemmele P, Hader Y, Weiss TS, Buechler C. Manganese superoxide dismutase is reduced in the liver of male but not female humans and

rodents with non-alcoholic fatty liver disease. Experimental and molecular pathology. 2013; 95:330–335. [PubMed: 24161595]

20. Miquilena-Colina ME, Lima-Cabello E, Sanchez-Campos S, Garcia-Mediavilla MV, Fernandez-Bermejo M, Lozano-Rodriguez T, Vargas-Castrillon J, Buque X, Ochoa B, Aspichueta P, Gonzalez-Gallego J, Garcia-Monzon C. Hepatic fatty acid translocase CD36 upregulation is associated with insulin resistance, hyperinsulinaemia and increased steatosis in non-alcoholic steatohepatitis and chronic hepatitis C. Gut. 2011; 60:1394–1402. [PubMed: 21270117]
21. Fernandez-Hernando C, Moore KJ. MicroRNA modulation of cholesterol homeostasis. Arteriosclerosis, thrombosis, and vascular biology. 2011; 31:2378–2382.
22. Frank PG, Pavlides S, Cheung MW, Daumer K, Lisanti MP. Role of caveolin-1 in the regulation of lipoprotein metabolism. American journal of physiology Cell physiology. 2008; 295:C242–248. [PubMed: 18508910]
23. Motoshima H, Goldstein BJ, Igata M, Araki E. AMPK and cell proliferation--AMPK as a therapeutic target for atherosclerosis and cancer. The Journal of physiology. 2006; 574:63–71. [PubMed: 16613876]
24. Docke S, Lock JF, Birkenfeld AL, Hoppe S, Lieske S, Rieger A, Raschzok N, Sauer IM, Florian S, Osterhoff MA, Heller R, Herrmann K, Lindenmuller S, Horn P, Bauer M, Weickert MO, Neuhaus P, Stockmann M, Mohlig M, Pfeiffer AF, von Loeffelholz C. Elevated hepatic chemerin mRNA expression in human non-alcoholic fatty liver disease. European journal of endocrinology / European Federation of Endocrine Societies. 2013; 169:547–557. [PubMed: 23935128]
25. Krautbauer S, Wanninger J, Eisinger K, Hader Y, Beck M, Kopp A, Schmid A, Weiss TS, Dorn C, Buechler C. Chemerin is highly expressed in hepatocytes and is induced in non-alcoholic steatohepatitis liver. Experimental and molecular pathology. 2013; 95:199–205. [PubMed: 23906870]
26. Wang N, Arai T, Ji Y, Rinninger F, Tall AR. Liver-specific overexpression of scavenger receptor BI decreases levels of very low density lipoprotein ApoB, low density lipoprotein ApoB, and high density lipoprotein in transgenic mice. J Biol Chem. 1998; 273:32920–32926. [PubMed: 9830042]
27. Hu Z, Hu J, Zhang Z, Shen WJ, Yun CC, Berlot CH, Kraemer FB, Azhar S. Regulation of expression and function of scavenger receptor class B, type I (SR-BI) by Na+/H+ exchanger regulatory factors (NHERFs). J Biol Chem. 2013; 288:11416–11435. [PubMed: 23482569]
28. Chiang JY. Bile acids: regulation of synthesis. Journal of lipid research. 2009; 50:1955–1966. [PubMed: 19346330]
29. Wood P, Mulay V, Darabi M, Chan KC, Heeren J, Pol A, Lambert G, Rye KA, Enrich C, Grewal T. Ras/mitogen-activated protein kinase (MAPK) signaling modulates protein stability and cell surface expression of scavenger receptor SR-BI. J Biol Chem. 2011; 286:23077–23092. [PubMed: 21525007]
30. Heimerl S, Liebisch G, Le Lay S, Bottcher A, Wiesner P, Lindtner S, Kurzchalia TV, Simons K, Schmitz G. Caveolin-1 deficiency alters plasma lipid and lipoprotein profiles in mice. Biochem Biophys Res Commun. 2008; 367:826–833. [PubMed: 18191037]
31. Subbaiah PV, Jiang XC, Belikova NA, Aizezi B, Huang ZH, Reardon CA. Regulation of plasma cholesterol esterification by sphingomyelin: effect of physiological variations of plasma sphingomyelin on lecithin-cholesterol acyltransferase activity. Biochimica et biophysica acta. 2012; 1821:908–913. [PubMed: 22370449]
32. Subbaiah PV, Gesquiere LR, Wang K. Regulation of the selective uptake of cholesteryl esters from high density lipoproteins by sphingomyelin. Journal of lipid research. 2005; 46:2699–2705. [PubMed: 16162942]
33. Subbaiah PV, Horvath P, Achar SB. Regulation of the activity and fatty acid specificity of lecithin-cholesterol acyltransferase by sphingomyelin and its metabolites, ceramide and ceramide phosphate. Biochemistry. 2006; 45:5029–5038. [PubMed: 16605271]
34. Li Y, Dong J, Ding T, Kuo MS, Cao G, Jiang XC, Li Z. Sphingomyelin synthase 2 activity and liver steatosis: an effect of ceramide-mediated peroxisome proliferator-activated receptor gamma2 suppression. Arteriosclerosis, thrombosis, and vascular biology. 2013; 33:1513–1520.
35. Benharouga M, Sharma M, So J, Haardt M, Drzymala L, Popov M, Schwapach B, Grinstein S, Du K, Lukacs GL. The role of the C terminus and Na+/H+ exchanger regulatory factor in the

functional expression of cystic fibrosis transmembrane conductance regulator in nonpolarized cells and epithelia. J Biol Chem. 2003; 278:22079–22089. [PubMed: 12651858]

36. Saras J, Heldin CH. PDZ domains bind carboxy-terminal sequences of target proteins. Trends in biochemical sciences. 1996; 21:455–458. [PubMed: 9009824]
37. Neufeld EB, Remaley AT, Demosky SJ, Stonik JA, Cooney AM, Comly M, Dwyer NK, Zhang M, Blanchette-Mackie J, Santamarina-Fojo S, Brewer HB Jr. Cellular localization and trafficking of the human ABCA1 transporter. J Biol Chem. 2001; 276:27584–27590. [PubMed: 11349133]
38. Fitzgerald ML, Okuhira K, Short GF 3rd, Manning JJ, Bell SA, Freeman MW. ATP-binding cassette transporter A1 contains a novel C-terminal VFVNFA motif that is required for its cholesterol efflux and ApoA-I binding activities. J Biol Chem. 2004; 279:48477–48485. [PubMed: 15347662]
39. Zachwieja JJ. Exercise as treatment for obesity. Endocrinology and metabolism clinics of North America. 1996; 25:965–988. [PubMed: 8977056]
40. Rigotti A, Trigatti BL, Penman M, Rayburn H, Herz J, Krieger M. A targeted mutation in the murine gene encoding the high density lipoprotein (HDL) receptor scavenger receptor class B type I reveals its key role in HDL metabolism. Proceedings of the National Academy of Sciences of the United States of America. 1997; 94:12610–12615. [PubMed: 9356497]
41. Li G, Thomas AM, Williams JA, Kong B, Liu J, Inaba Y, Xie W, Guo GL. Farnesoid X receptor induces murine scavenger receptor Class B type I via intron binding. PloS one. 2012; 7:e35895. [PubMed: 22540009]
42. Zou Y, Du H, Yin M, Zhang L, Mao L, Xiao N, Ren G, Zhang C, Pan J. Effects of high dietary fat and cholesterol on expression of PPAR alpha, LXR alpha, and their responsive genes in the liver of apoE and LDLR double deficient mice. Molecular and cellular biochemistry. 2009; 323:195–205. [PubMed: 19067122]
43. Leiva A, Verdejo H, Benitez ML, Martinez A, Busso D, Rigotti A. Mechanisms regulating hepatic SR-BI expression and their impact on HDL metabolism. Atherosclerosis. 2011; 217:299–307. [PubMed: 21741044]
44. Martinez-Beamonte R, Lou-Bonafonte JM, Martinez-Gracia MV, Osada J. Sphingomyelin in high-density lipoproteins: structural role and biological function. International journal of molecular sciences. 2013; 14:7716–7741. [PubMed: 23571495]
45. Oorni K, Hakala JK, Annila A, Ala-Korpela M, Kovanen PT. Sphingomyelinase induces aggregation and fusion, but phospholipase A2 only aggregation, of low density lipoprotein (LDL) particles. Two distinct mechanisms leading to increased binding strength of LDL to human aortic proteoglycans. J Biol Chem. 1998; 273:29127–29134. [PubMed: 9786921]
46. Schlitt A, Hojjati MR, von Gizycki H, Lackner KJ, Blankenberg S, Schwaab B, Meyer J, Rupprecht HJ, Jiang XC. Serum sphingomyelin levels are related to the clearance of postprandial remnant-like particles. Journal of lipid research. 2005; 46:196–200. [PubMed: 15547302]
47. Ridgway ND. Inhibition of acyl-CoA:cholesterol acyltransferase in Chinese hamster ovary (CHO) cells by short-chain ceramide and dihydroceramide. Biochimica et biophysica acta. 1995; 1256:39–46. [PubMed: 7742354]
48. Dong J, Liu J, Lou B, Li Z, Ye X, Wu M, Jiang XC. Adenovirus-mediated overexpression of sphingomyelin synthases 1 and 2 increases the atherogenic potential in mice. Journal of lipid research. 2006; 47:1307–1314. [PubMed: 16508036]
49. Guegan JP, Fremin C, Baffet G. The MAPK MEK1/2-ERK1/2 Pathway and Its Implication in Hepatocyte Cell Cycle Control. International journal of hepatology. 2012; 2012:328372. [PubMed: 23133759]
50. Burns KA, Vanden Heuvel JP. Modulation of PPAR activity via phosphorylation. Biochimica et biophysica acta. 2007; 1771:952–960. [PubMed: 17560826]
51. Lan D, Silver DL. Fenofibrate induces a novel degradation pathway for scavenger receptor B-I independent of PDZK1. J Biol Chem. 2005; 280:23390–23396. [PubMed: 15837786]
52. Tsukamoto K, Buck L, Inman W, Griffith L, Kocher O, Krieger M. Challenges in using cultured primary rodent hepatocytes or cell lines to study hepatic HDL receptor SR-BI regulation by its cytoplasmic adaptor PDZK1. PloS one. 2013; 8:e69725. [PubMed: 23936087]

- Mice deficient for alpha and beta 2 syntrophin have normal serum insulin
- Hepatic ABCA1 protein is similar to wild type mice
- Increased ERK1/2 seems to contribute to low hepatic SR-BI
- Sphingomyelin is reduced in the liver and serum of the knock-out mice
- Hepatic but not serum cholesterol is lower in the knock-out animals

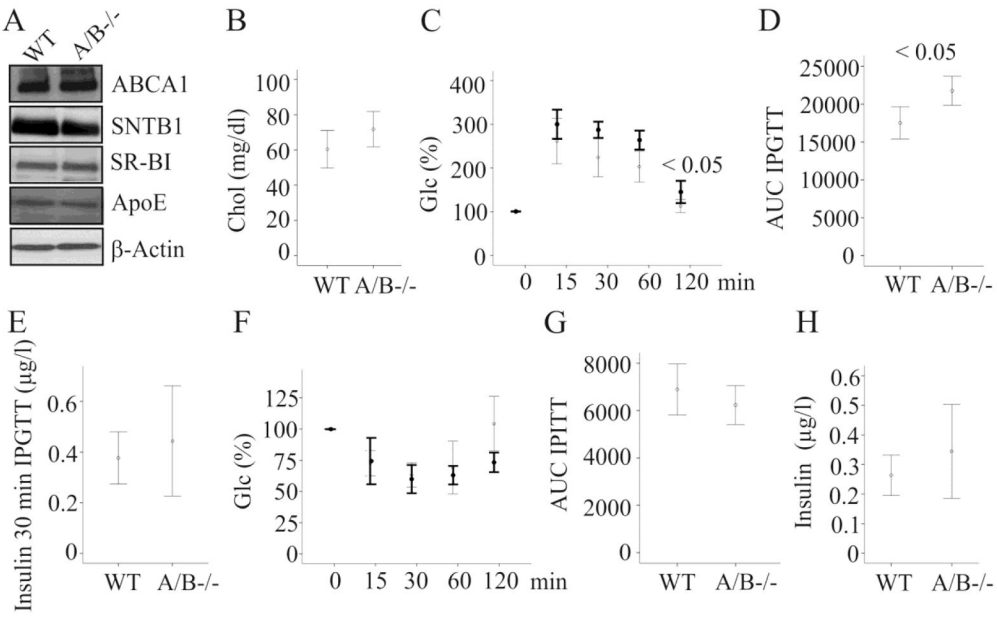

Figure 1. ABCA1, intraperitoneal glucose and insulin tolerance tests (IPGTT, IPITT) and insulin in SNTA/B2−/− (A/B−/−) mice fed a SD

(A) ABCA1, SNTB1, SR-BI, ApoE and β-actin in the liver of wild type (WT) and SNTA/B2−/− mice. (B) Serum cholesterol in 6 WT and 5 SNTA/B2−/− mice. (C) IPGTT in 6 WT and 3 SNTA/B2−/− mice. Data of the knock-out mice are shown in bold. (D) Area under the curve (AUC) of glucose shown in C. (E) Serum insulin of the animals described in C 30 minutes after glucose injection. (F) IPITT in 6 WT and 3 SNTA/B2−/− mice. Data of the knock-out mice are shown in bold. (G) AUC of IPITT. (H) Fasting insulin measured in serum of 9 WT and 10 SNTA/B2−/− mice.

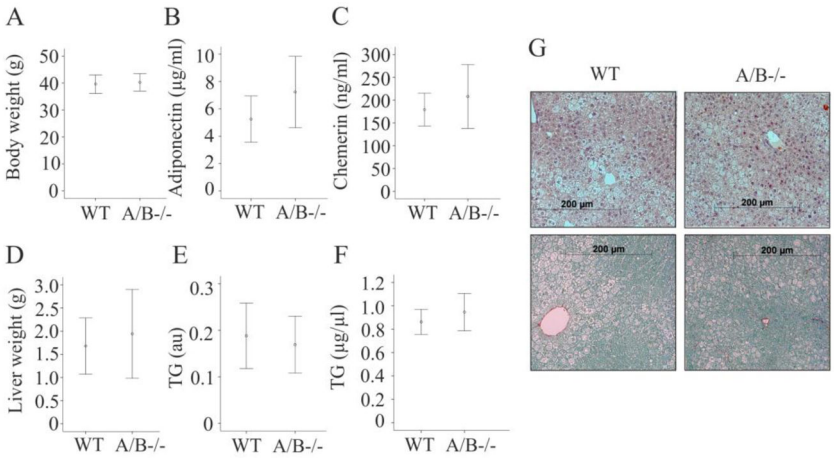

Figure 2. Body weight, adipokines and triglycerides in SNTA/B2−/− (A/B−/−) mice fed a HFD

(A) Body weight of 8 WT and 8 SNTA/B2−/− mice after 25 weeks HFD feeding. (B) Serum adiponectin of 7 WT and 8 SNTA/B2−/− mice. (C) Serum chemerin of 7 WT and 8 SNTA/B2−/− mice. (D) Liver weight of 8 WT and 8 SNTA/B2−/− mice after 25 weeks HFD feeding. (E) Liver triglycerides of these mice, au arbitrary units. (F) Serum triglycerides of these mice. (G) H&E and Sirius Red stained liver of a WT and a SNTA/B2−/− mouse.

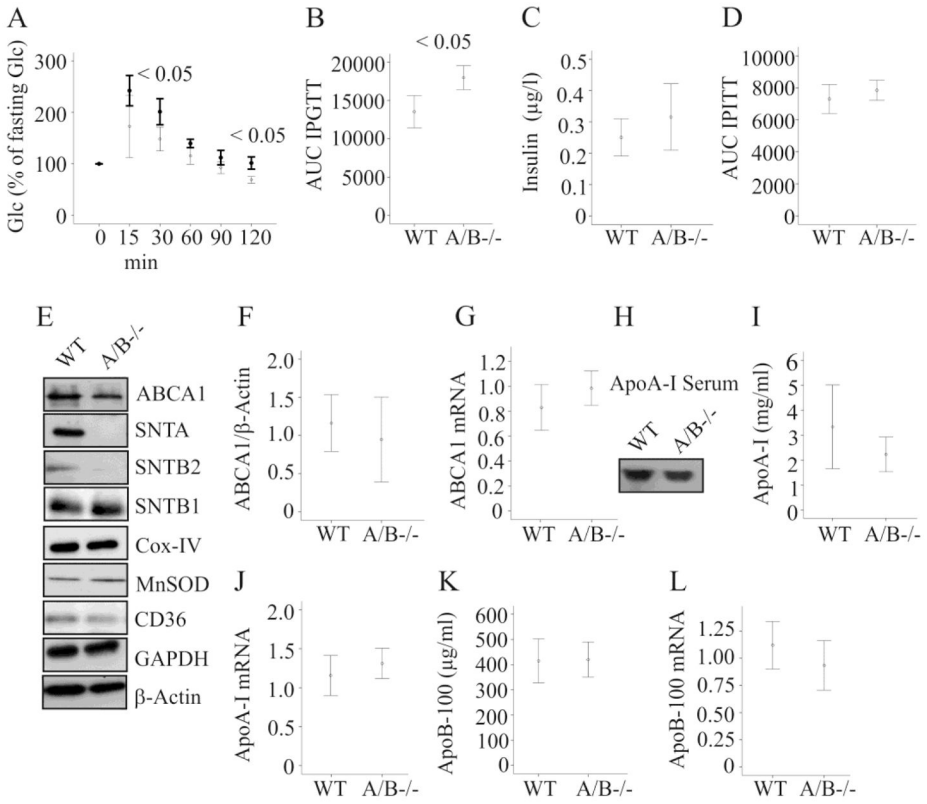

Figure 3. Intraperitoneal glucose tolerance test (IPGTT), insulin, hepatic ABCA1 and serum apolipoproteins in SNTA/B2−/− (A/B−/−) mice fed a HFD

(A) IPGTT in 5 WT and 5 SNTA/B2−/− mice fed a HFD for 16 weeks. Data of the knock-out mice are shown in bold. (B) Area under the curve (AUC) of IPGTT shown in A. (C) Fasting insulin measured in serum of 5 WT and 4 SNTA/B2−/− mice fed a HFD for 25 weeks (D) AUC of IPITT of 5 wild type and 5 SNTA/B−/− mice. (E) ABCA1, SNTA, SNTB2, SNTB1, Cox-IV, MnSOD, CD36, GAPDH and β-actin in the liver of WT and SNTA/B2−/− mice fed a HFD for 25 weeks. (F) ABCA1 protein in the liver of 8 WT and 8 SNTA/B2−/− mice. (G) ABCA1 mRNA in the liver of 8 WT and 7 SNTA/B2−/− mice. (H) Immunoblot of ApoA-I in serum of a WT and a double knock-out mouse. (I) ApoA-I in the serum of 8 WT and 8 SNTA/B2−/− mice. (J) ApoA-I mRNA in the liver of 8 WT and 7 SNTA/B2−/− mice. (K) ApoB-100 in the serum of 6 WT and 5 SNTA/B2−/− mice. (L) ApoB-100 mRNA in the liver of 8 WT and 7 SNTA/B2−/− mice.

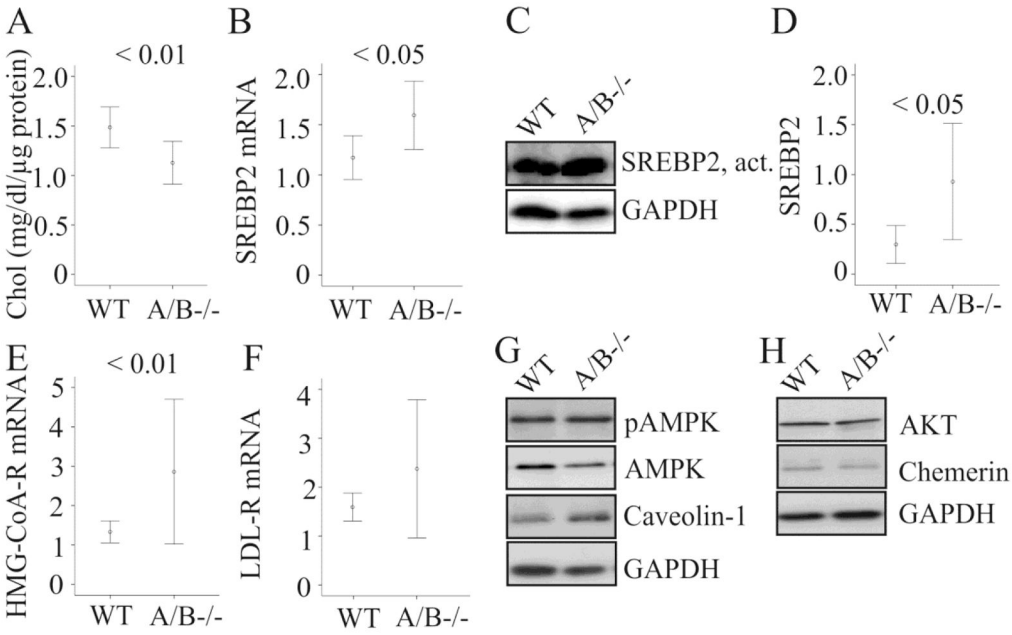

Figure 4. Hepatic cholesterol and proteins with a role in cholesterol homeostasis in SNTA/B2−/− (A/B−/−) mice fed a HFD

(A) Liver cholesterol (Chol) measured with a commercial assay and normalized to total protein in 8 WT and 8 SNTA/B2−/− mice fed a HFD for 25 weeks. (B) SREBP2 mRNA in the liver of 8 WT and 7 SNTA/B2−/− mice fed a HFD for 25 weeks. (C) Active SREBP2 protein in the liver (D) Quantification of active SREBP2 protein in the liver of 7 WT and 7 SNTA/B2−/− mice fed a HFD for 25 weeks. (E) HMG-CoA-R mRNA in the liver of 8 WT and 7 SNTA/B2−/− mice fed a HFD for 25 weeks. (F) LDL-R mRNA in the liver of these mice. (G) pAMPK, AMPK and caveolin-1 in the liver of a wild type and a SNTA/B2 null mouse. (H) AKT and chemerin in the liver of a wild type and a SNTA/B2 null mouse.

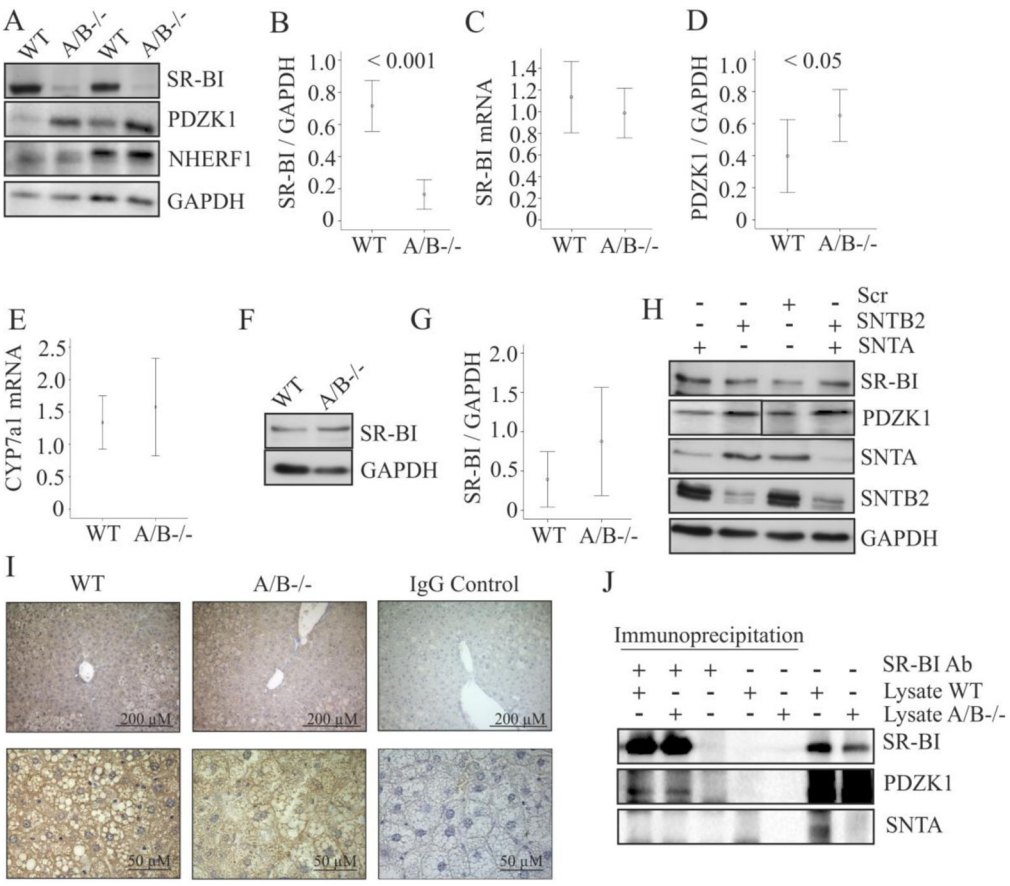

Figure 5. SR-BI in the liver, brown adipose tissue and siRNA transfected Hepa 1-6 cells

(A) SR-BI, PDZK1 and NHERF1 in the liver of 2 wild type and 2 SNTA/B2 null mice. (B) SR-BI protein in the liver of 8 WT and 8 SNTA/B2−/− mice fed a HFD for 25 weeks. (C) SR-BI mRNA in the liver of 8 WT and 7 SNTA/B2−/− mice fed a HFD for 25 weeks. (D) PDZK1 protein in the liver of 7 WT and 7 SNTA/B2−/− mice fed a HFD for 25 weeks. (E) CYP7a1 mRNA in the liver of 8 WT and 7 SNTA/B2−/− mice. (F) SR-BI in brown adipose tissue of a wild type and a SNTA/B2 null mouse fed a HFD for 25 weeks. (G) SR-BI protein in brown adipose tissue of 8 WT and 8 SNTA/B2−/− mice fed a HFD for 25 weeks. (H) SR-BI, PDZK1, SNTA and SNTB2 in Hepa1-6 cells transfected with scrambled (Scr) siRNA, SNTA siRNA, SNTB2 siRNA or both. (I) PDZK1 in the liver of wild type and SNTA/B−/− mice. Original magnification of the upper panels was 20-fold and of the lower panels 60-fold. The respective IgG isotype controls are shown on the right. (J) SR-BI was immunoprecipitated in liver lysates of WT and SNTA/B2−/− mice. SR-BI, PDZK1 and SNTA were analyzed by immunoblot in the immunoprecipitates, respective control experiments and the liver lysates used.

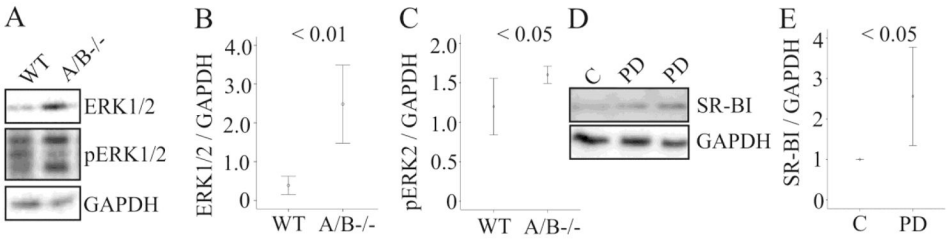

Figure 6. ERK1/2 in the liver and effect of ERK1/2 inhibitor on hepatocyte SR-BI

(A) ERK1/2 and pERK1/2 in the liver of a wild type and a SNTA/B2 null mice. (B) ERK1/2 protein in the liver of 7 WT and 7 SNTA/B2−/− mice fed a HFD for 25 weeks. (C) pERK2 protein in the liver of 6 WT and 5 SNTA/B2−/− mice. (D) SR-BI in primary hepatocytes incubated with the ERK1/2 inhibitor PD98059 for 24 h. (E) Quantification of the data of three experiments partly shown in D. Controls were set to 1.

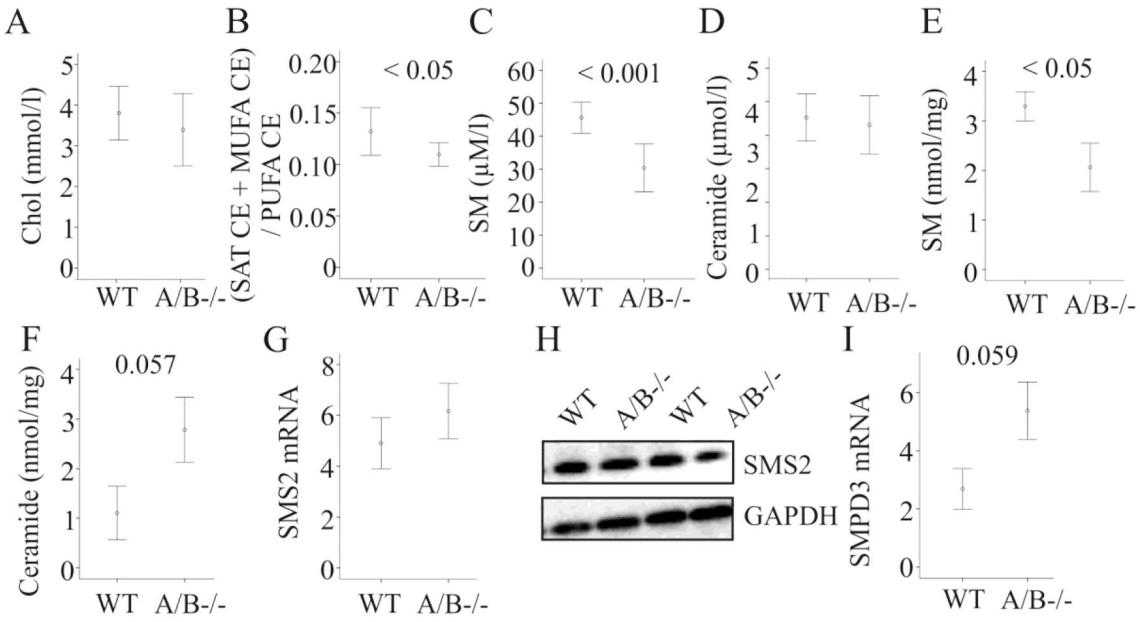

Figure 7. Cholesterol, sphingomyelin and ceramide in SNTA/B2−/− (A/B−/−) mice fed a HFD

(A) Serum cholesterol measured in 8 WT and 8 SNTA/B2−/− mice fed a HFD for 25 weeks by ESI-MS/MS. (B) Ratio of saturated (SAT) and monounsaturated (MUFA) to polyunsaturated (PUFA) cholesteryl ester (CE) species in the serum of these mice. (C) Serum sphingomyelin (SM) measured in 8 WT and 8 SNTA/B2−/− mice fed a HFD for 25 weeks. (D) Serum ceramide measured in 8 WT and 8 SNTA/B2−/− mice fed a HFD for 25 weeks. (E) Hepatic sphingomyelin (SM) measured in 4 WT and 4 SNTA/B2−/− mice fed a HFD for 25 weeks. (F) Hepatic ceramide measured in 4 WT and 4 SNTA/B2−/− mice fed a HFD for 25 weeks. (G) SMS2 mRNA in the liver of 8 wild type and 7 SNTA/B2 null mice. (H) SMS2 protein in the liver of two wild type and two SNTA/B2 null mice. (I) SMPD3 mRNA in the liver of 8 wild type and 6 SNTA/B2 null mice.

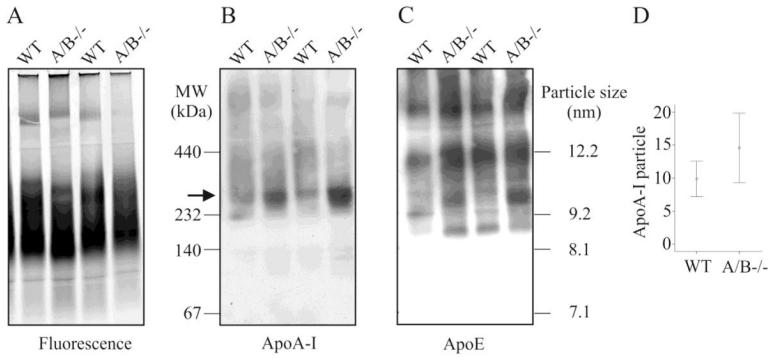

Figure 8. Distribution of lipoproteins

(A) Plasma samples stained with a lipophilic dialkylaminostyryl fluorophore. (B) Plasma samples were analyzed for distribution of ApoA-I and (C) ApoE. (D) Quantification of the ApoA-I particles marked by an arrow in B in plasma of 6 wild type and 7 SNTA/B2−/− animals.